Mn^{2+} Binding to Factor VIII Subunits and Its Effect on Cofactor Activity†

Hironao Wakabayashi, Zhu Zhen, Kyla M. Schmidt, and Philip J. Fay*

Department of Biochemistry and Biophysics, University of Rochester School of Medicine, 601 Elmwood Avenue, Rochester, New York, 14642

Received July 10, 2002; Revised Manuscript Received November 11, 2002

ABSTRACT: Metal ions, such as Ca^{2+} and Mn^{2+}, are necessary for the generation of cofactor activity following reconstitution of factor VIII from its isolated light chain (LC) and heavy chain (HC). Titration of EDTA-treated factor VIII with Mn^{2+} showed saturable binding with high affinity ($K_d = 5.7 \pm 2.1$ μM) as detected using a factor Xa generation assay. No significant competition between Ca^{2+} and Mn^{2+} for factor VIII binding ($K_i = 4.6$ mM) was observed as measured by equilibrium dialysis using 20 μM Ca^{2+} and 8 μM factor VIII in the presence of 0−1 mM Mn^{2+}. The intersubunit affinity measured by fluorescence energy transfer of an acrylodan-labeled LC (fluorescence donor) and fluorescein-labeled HC (fluorescence acceptor) in the presence of 20 mM Mn^{2+} ($K_d = 53.0 \pm 17.1$ nM) was not significantly different from the affinity value previously obtained in the absence of metal ion ($K_d = 53.8 \pm 14.2$ nM). The sensitization of phosphorescence of Tb^{3+} bound to factor VIII subunits was utilized to detect Mn^{2+} binding to the subunits. Mn^{2+} inhibited the phosphorescence of Tb^{3+} bound to HC and LC, as well as the HC-derived A1 and A2 subunits with a relatively wide range of estimated inhibition constant values (K_i values = 169−1147 μM), whereas Ca^{2+} showed no effect on Tb^{3+} phosphorescence. These results suggest that factor VIII cofactor activity can be generated by Mn^{2+} binding to site(s) on factor VIII that are different from the high-affinity Ca^{2+} binding site. However, like Ca^{2+}, Mn^{2+} did not alter the affinity for HC and LC association. Thus, Mn^{2+} appears to generate factor VIII cofactor activity by a similar mechanism as observed for Ca^{2+} following its association at nonidentical sites on the protein.

Factor VIII, a plasma protein that participates in the blood coagulation cascade, is decreased or defective in individuals with hemophilia A. Factor VIII functions as a cofactor for the serine protease factor IXa in the surface-dependent conversion of zymogen factor X to the serine protease, factor Xa (*1*, *2*). Deficiency of factor VIII causes marked reduction of factor IXa activity and in subsequent rates of factor Xa generation.

Factor VIII is synthesized as an ∼300-kDa single chain precursor protein (*3*, *4*) with domain structure A1−A2−B−A3−C1−C2 (*5*). Factor VIII is processed to a series of divalent metal ion-linked heterodimers (*6*−*8*) by cleavage at the B−A3 junction, generating a heavy chain (HC)[1] minimally represented by the Al−A2 domains, and a light chain (LC) consisting of the A3−C1−C2 domains. Metal ions play an important role in regulating factor VIII structure and activity. The A domains of factor VIII share homology with the A domains of factor V and the copper-binding protein, ceruloplasmin (*9*). One mole of copper has been identified in factor VIII (*10*, *11*).

Factor VIII is inactivated by EDTA, which facilitates dissociation of the HC and LC (*6*, *8*). Factor VIII can be reconstituted by combining the isolated subunits in the presence of Ca^{2+} or Mn^{2+} (*12*−*14*). In addition, the presence of low levels of Cu^{+} or Cu^{2+} stimulate this effect (*11*, *15*). Thus, it was thought that the linkage of HC and LC by a metal ion (Ca^{2+}, Mn^{2+}, or Cu^{2+}) formed an active heterodimer. This interpretation was consistent with studies examining the reconstitution of factor Va from isolated subunits by Ca^{2+} or Mn^{2+} (*16*, *17*). We recently evaluated metal ion-dependent and -independent association of factor VIII chains (*18*). In the absence of metal ion, LC and HC combine to form an inactive heterodimer as demonstrated by fluorescence energy transfer. Ca^{2+} has little effect on intersubunit affinity yet it converts the inactive dimer to an active, although low specific activity, form. In contrast, Cu^{2+} enhances the intersubunit affinity ∼100-fold but yields a dimer that lacks activity. However, the presence of both metal ions results in a high intersubunit affinity and yields a high specific activity factor VIII. A recent study on the role of Ca^{2+} in factor VIII indicated that Ca^{2+} binding to both factor VIII subunits was required for the generation of cofactor activity (*19*). These studies also demonstrated that a local conformational change in response to Ca^{2+} binding correlates with formation of the active cofactor.

Although Mn^{2+} seems to affect the reconstitution of factor VIII activity in a manner similar to that observed for Ca^{2+}, little quantitative information is available on the interaction

† This work was supported by NIH Grants HL 38199 and HL 30616.

* Address correspondence to this author. Tel: (585) 275-6576. Fax: (585) 473-4314. E-mail: philip_fay@urmc.rochester.edu.

[1] Abbreviations: HC, factor VIII heavy chain; LC, factor VIII light chain; EGTA, ethylene glycol bis(β-aminoethyl ether)-*N*,*N*,*N*′,*N*′-tetraacetic acid; EDTA, ethylenediamine tetraacetic acid; BAPTA, 1,2-bis(*o*-aminophenoxy)-ethane-*N*,*N*,*N*′,*N*′-tetraacetic acid; MES, 2-[*N*-morpholino]ethanesulfonic acid; HEPES, *N*-[2-hydroxyethyl]piperazine-*N*′-[2-ethanesulfonic acid]; PS, phosphotidylserine; PC, phosphotidylcholine; and PE, phosphotidylethanolamine.

10.1021/bi026430e CCC: $25.00
Published on Web 12/10/2002

of Mn^{2+} with factor VIII (subunits). Furthermore, the characterization of Mn^{2+} binding to factor VIII would help to clarify the mechanisms by which selected divalent metal ions modulate cofactor activity. In the current study we demonstrate that, similar to Ca^{2+}, Mn^{2+} possesses a high-affinity binding site for factor VIII that does not influence the affinity of the HC and LC in the factor VIII heterodimer. However, several lines of evidence show that the metal ions occupy nonidentical sites, suggesting that occupancy of either type of site(s) by the respective divalent metal ion drives a conformational change that yields the active cofactor.

MATERIALS AND METHODS

Reagents. Recombinant factor VIII preparations (Kogenate) were a gift from Dr. Lisa Regan of Bayer Corporation (Berkeley, CA). Purified recombinant factor VIII was also a generous gift from Debra Pittman of the Genetics Institute (Cambridge, MA). Phospholipid vesicles containing 20% PS, 40% PC, and 40% PE were prepared using octylglucoside as described previously (*20*). The reagents α-thrombin, factor IXaβ, factor X, and factor Xa (Enzyme Research Laboratories, South Bend, IN); hirudin, phospholipids, $MnCl_2$, and $TbCl_3$ (Sigma, St. Louis, MO); the chromogenic Xa substrate S-2765 (*N*-α-benzyloxycarbonyl-D-arginyl-L-glycyl-L-arginyl-*p*-nitroanilide-dihydrochloride; DiaPharma, West Chester, OH); ^{45}Ca (Amersham-pharmacia Biotech, Piscataway, NJ); and 5,5′-dibromoBAPTA (Molecular Probes, Eugene, OR) were purchased from the indicated vendors.

Preparation of Factor VIII and Subunits. Factor VIII (Kogenate) was dissolved in 20 mM HEPES, 0.3 M KCl, and 0.01% Tween-20 (pH 7.2), further concentrated using a CentriPlus concentrator (Millipore, Bedford, MA), dialyzed into the same buffer, and stored at −80 °C. Factor VIII LC, HC, A1, and A2 subunits were isolated from factor VIII as previously described (*21*), dialyzed into 10 mM MES, 0.3 M KCl, and 0.01% Tween-20 (pH 6.5) and stored at −80 °C.

Preparation of Mn^{2+}−EGTA Buffer with Specified Free Mn^{2+}. A Mn^{2+}−EGTA buffer with free Mn^{2+} concentrations ranging between 1 μM and 20 mM in the presence of 5 mM EGTA was made based upon the apparent K_d for the Mn^{2+}−EGTA complex. The apparent K_d for the Mn^{2+}−EGTA complex in 10 mM MES and 0.3 M KCl (pH 6.5) was obtained experimentally using 5,5′-dibromoBAPTA as a probe (*22*). A two-step method was employed based on the procedure performed by Linse et al. (*23*). In the first step, the affinity of 5,5′-dibromoBAPTA for Mn^{2+} was determined by titration of a fixed concentration of the probe (0.75 μM) with the metal ion and was added in 0.1 μM increments, and absorbance was monitored at 263 nm (Figure 1A). The K_d for 5,5′-dibromoBAPTA−Mn^{2+} binding (K_B) was estimated by subsequent curve fitting (see below; total EGTA concentration = 0). The second step of the procedure examined competition (monitored at 263 nm) of the 5,5′-dibromoBAPTA−Mn^{2+} complex (5 μM) with variable concentrations of EGTA (Figure 1B) to estimate the K_d for the Mn^{2+}−EGTA complex (K_E). The changes in the concentrations of total 5,5′-dibromoBAPTA ($tBrB_i$), total Mn^{2+} (tMn^{2+}), and total EGTA ($tEGTA_i$) because of the change in volume at titration point *i* were corrected, and for each

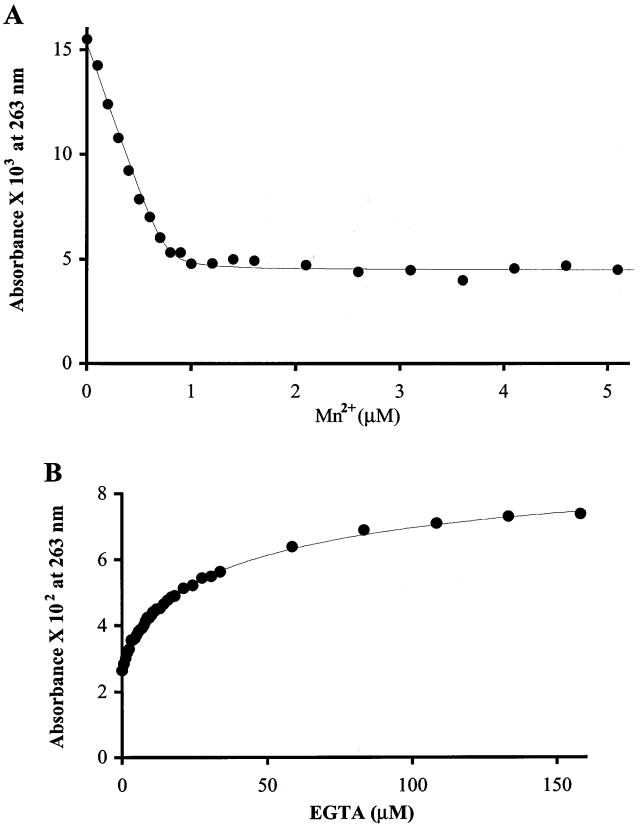

FIGURE 1: Determination of the affinity of Mn^{2+} for EGTA using 5,5′-dibromoBAPTA. (A) Detection of Mn^{2+} binding to 5,5′-dibromoBAPTA. Mn^{2+} was incrementally added to 5,5′-dibromoBAPTA (0.75 μM), and the absorbance at 263 nm was measured. The line was drawn from the curve fit as described in Materials and Methods. The dissociation constant for 5,5′-dibromoBAPTA and Mn^{2+} binding from the curve fitting was determined as 0.0095 μM. (B) Competition of Mn^{2+}-5,5′-dibromoBAPTA binding using EGTA. EGTA was incrementally added to a solution containing 5,5′-dibromoBAPTA and Mn^{2+} (5 μM each), and the absorbance at 263 nm was measured. Each point represents the average value of triplicated experiments. The line was drawn from the curve fit as described in Materials and Methods. The dissociation constant for EGTA and Mn^{2+} was determined to be 0.12 μM.

set of assigned parameters the Newton−Raphson method was used to solve the free Mn^{2+} concentration (= $[Mn^{2+}]$) based on the following equation:

$$tMn_i - [Mn^{2+}] - \frac{tBrB_i[Mn^{2+}]}{[Mn^{2+}] + K_B} - \frac{tEGTA_i[Mn^{2+}]}{[Mn^{2+}] + K_E} = 0 \quad (1)$$

where K_B is the dissociation constant for 5,5′-dibromoBAPTA−Mn^{2+} binding, and K_E is the dissociation constant for EGTA−Mn^{2+} binding. Subsequent determination of the K_B or K_E was done by iterating the variable parameters until the minimum error square sum (ESS) was found using the equation below. This procedure is based on numerical evaluation of the first and second derivatives of ESS with respect to each parameter.

$$Abs_{calculated,i} = \left[AMAX - (AMAX - AMIN)\frac{[Mn^{2+}]}{[Mn^{2+}] + K_B}\right] \cdot \frac{tBrB_i}{tBrB_1} \quad (2)$$

where *AMAX* is the absorbance of 5,5′-dibromoBAPTA in the absence of metal ion, *AMIN* is the absorbance of Mn^{2+}-saturated 5,5′-dibromoBAPTA, $Abs_{calculated,i}$ is the calculated absorbance at point *i*, and $Abs_{measured,i}$ is the measured absorbance at point *i*.

Factor VIII Activity Titration by Mn^{2+}. HC (100 nM) and LC (100 nM) were recombined in each Mn^{2+}−EGTA buffer (free Mn^{2+} concentrations between 1 μM and 20 mM) at 23 °C for 18 h, and resultant factor VIII activity was measured using the factor Xa generation assay as described below. Nonlinear least-squares regression analysis was performed according to a single-site binding model using the following equation:

$$Activity = \frac{A\cdot[Mn^{2+}]}{K_d + [Mn^{2+}]} \quad (3)$$

where *A* is a constant reflecting maximal activity, and K_d is the dissociation constants.

Factor Xa Generation Assays. The rate of conversion of factor X to factor Xa was monitored in a purified system (*24*) according to the method described previously (*18*, *19*), and the activity was expressed as the amount of factor Xa generated (nM) per minute and converted to the value per nanomolar LC.

Equilibrium Dialysis Using ^{45}Ca. Equilibrium dialysis was performed as described previously (*19*). Factor VIII (8 μM) in 20 mM HEPES (pH 7.2), 0.3 M KCl, and 0.01% Tween-20 was added to one side of the equilibrium dialysis apparatus with 20 μM Ca^{2+} containing ∼2000 Bq ^{45}Ca in the presence of 0−1 mM Mn^{2+}. After a 48-h incubation at 23 °C, ^{45}Ca radioactivity was measured by liquid scintillation counting, and the amounts of free Ca^{2+} and factor VIII-bound Ca^{2+} were calculated. To estimate the inhibition constant (K_i) for Mn^{2+} on Ca^{2+} binding to factor VIII, a similar procedure for the calculation of the dissociation constant for Mn^{2+}−EGTA binding described above was utilized.

Fluorescence Energy Transfer. Fluorescence energy transfer was employed to detect the effect of Mn^{2+} on HC and LC association according to methods as described previously (*18*) substituting 20 mM Mn^{2+} in place of 25 mM Ca^{2+}.

Measurement of Mn^{2+} Binding to Factor VIII and Its Subunits Using Tb^{3+} Phosphorescence. Mn^{2+} binding to factor VIII and its subunits was measured by detecting reduction of the phosphorescence signal from protein-bound Tb^{3+} (*25*). The protein−Tb^{3+} ion complex was excited at 295 nm. Resultant sensitized phosphorescence derived from energy transfer from excited aromatic amino acids was recorded from 520 to 560 nm (bandwidth 4 nm) using an Aminco-Bowman Series 2 Luminescence Spectrometer (Thermo Spectronic, Rochester, NY). The phosphorescence intensity was recorded by averaging the values from 15 measurements taken at a 30-ms interval. Each measurement was monitored for an 800-μs duration preceded by a 200-μs delay period following excitation.

Initially, factor VIII subunits (1−6 μM) were incubated with various concentrations of $TbCl_3$ (0−8 mM) for 18 h at 25 °C, and the Tb^{3+} binding to these proteins was evaluated. Nonlinear least-squares regression analysis was performed according to a single-site binding model and a two-site binding model (nonidentical and independent sites) using the equations

$$Phosphorescence(F) = \frac{F_{max}\cdot[Tb^{3+}]}{K_d + [Tb^{3+}]} \quad \text{and} \quad (4)$$

$$Phosphorescence(F) = [Tb^{3+}]\left(\frac{F_{max1}}{K_{d1} + [Tb^{3+}]} + \frac{F_{max2}}{K_{d2} + [Tb^{3+}]}\right), \text{ respectively,} \quad (5)$$

where $[Tb^{3+}]$ is free Tb^{3+} concentration; K_d, K_{d1}, and K_{d2} are the dissociation constants; and F_{max}, F_{max1}, and F_{max2} represent maximum phosphorescence signals when the sites are saturated by Tb^{3+}.

In a second series of reactions, the factor VIII subunits (1−6 μM) were incubated with $TbCl_3$ (0−2 mM) in the absence and presence of various concentrations of $MnCl_2$ (0−5 mM). Reactions were run for 18 h at 25 °C. Under these Tb^{3+} concentrations, the phosphorescence resulting from low-affinity binding sites, if any, was <15%. To evaluate Mn^{2+}-dependent inhibition of the high-affinity Tb^{3+} binding, each phosphorescence value was corrected as

$$F_H = F_T - F_L = F_T - \frac{F_{maxL}}{K_L + [Tb^{3+}]}$$

where F_H, F_T, and F_L represent the Tb^{3+} phosphorescence signal from the high-affinity site, the total Tb^{3+} phosphorescence, and the Tb^{3+} phosphorescence from the low-affinity site, respectively; and K_L and F_{maxL} are the dissociation constant and a maximum phosphorescence signal of the low-affinity Tb^{3+} binding site, respectively.

Mn^{2+} may inhibit Tb^{3+} phosphorescence by a competitive and/or indirect mechanism(s). From the general model of inhibition as described below (*26*), the total phosphorescence (*F*) can be calculated.

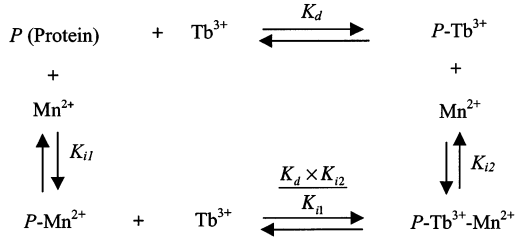

K_{i1} and K_{i2} are the dissociation constants for Mn^{2+} on Tb^{3+}-free and Tb^{3+}-bound protein (P). *F* is proportional to the concentration of free Tb^{3+}-bound protein [P−Tb^{3+}] or the concentration of free Tb^{3+} and Mn^{2+}-bound protein [P−Tb^{3+}−Mn^{2+}]; therefore,

$$F(Phosphorescence) = k\cdot[P - Tb^{3+}] + k\cdot[P - Tb^{3+} - Mn^{2+}]\cdot\alpha = k\cdot[P - Tb^{3+}]\cdot$$

$$\left[1 + \frac{\alpha\cdot[Mn^{2+}]}{K_{i2}}\right] = \frac{F_{max}\cdot\left[1 + \frac{a\cdot[Mn^{2+}]}{K_{i2}}\right]\cdot[Tb^{3+}]}{K_d\cdot\left[1 + \frac{[Mn^{2+}]}{K_{i1}}\right] + [Tb^{3+}]\cdot\left[1 + \frac{[Mn^{2+}]}{K_{i2}}\right]},$$

$$[P] \ll [Mn^{2+}] \text{ and } [Tb^{3+}] \quad (6)$$

where k is a constant, and α is the phosphorescence ratio reflecting the Tb^{3+}- and Mn^{2+}-bound complex ($P-Tb^{3+}-Mn^{2+}$) over the Tb^{3+}-bound complex ($P-Tb^{3+}$). For each factor VIII subunit, two variable ($[Tb^{3+}]$ and $[Mn^{2+}]$) nonlinear least-squares regression analyses were performed using eq 6.

Statistical Analysis. Nonlinear least-squares regression analysis was performed by Kaleidagraph (Synergy, Reading, PA) or SiamaPlot (Jandel Scientific, Chicago, IL), and the parameter values and their standard deviations were obtained. The best model to fit to the data was determined by a *F*-test comparing the sum of squares from each fitting. The percentage points (probability) for the *F*-distribution were calculated using Microsoft Excel.

RESULTS

Equilibrium Binding of Mn^{2+} to Factor VIII Detected by Functional Assay. Early experiments show that Mn^{2+}, as well as Ca^{2+}, reconstitute active factor VIII from isolated subunits (*12*). In a recent report (*19*), we quantitated the affinity of Ca^{2+} for factor VIII (chains) using a functional assay in the presence of known concentrations of free Ca^{2+}. These concentrations employed a $Ca^{2+}-$EGTA buffer system in which the free metal ion was known based upon the established affinity of Ca^{2+} for EGTA. Since this information is not available for the interaction of Mn^{2+} with EGTA, the affinity for this interaction was determined in a two-step process employing the probe, 5,5′-dibromoBAPTA, as described in Materials and Methods. This probe was selected for its high molar extinction coefficient and high affinity for Mn^{2+} (K_d = 0.0095 μM). However, the accuracy of the estimation was limited because of the relatively high ligand concentration used to determine the K_d for $Mn^{2+}-$5,5′-dibromoBAPTA binding. Using this method, the K_d for the $Mn^{2+}-$EGTA complex was estimated to be 0.12 μM. This value is ~40-fold lower than the calculated K_d for $Ca^{2+}-$EGTA binding (K_d = 4.66 μM) obtained under the equivalent reaction conditions.

On the basis of the above K_d value for the affinity of the $Mn^{2+}-$EGTA complex, a series of buffers varying in free Mn^{2+} (0−20 mM) in the presence of 5 mM EGTA were prepared. Reconstitution of factor VIII from isolated HC and LC was assessed as a function of free Mn^{2+}, and resultant activity was determined using a factor Xa generation assay. As shown in Figure 2, the extent of factor VIII activity was saturable with respect to Mn^{2+}, and peak activity levels were obtained at submillimolar concentrations of the metal ion. An estimated K_d for the factor VIII$-Mn^{2+}$ interaction was derived from curve fitting by nonlinear least-squares regression as described in Materials and Methods, using a one-site binding model (eq 3; $K_d = 5.7 \pm 2.1$ μM). Because of the limited accuracy of the K_d value for $Mn^{2+}-$5,5′-dibromoBAPTA, this estimated value may somewhat deviate from the true K_d for $Mn^{2+}-$factor VIII association. The maximum factor VIII activity obtained with a saturating level of Mn^{2+} concentration was ~1.4-fold higher than the value obtained following saturation by Ca^{2+} (*19*), and this observation was compatible with results from an earlier study (*12*). Control experiments indicated that final Mn^{2+} concentrations used in the reconstitution of the factor VIII subunits showed no effect on the factor Xa generation assay (data not shown).

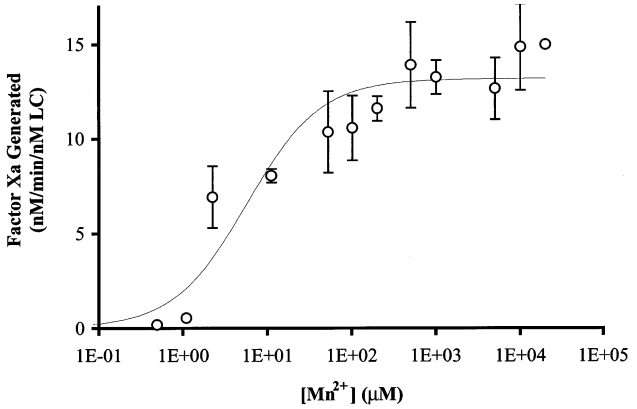

FIGURE 2: Equilibrium binding of Mn^{2+} to reconstituted factor VIII assessed by a functional assay. Mixtures of 100 nM LC, 100 nM HC, and the indicated amounts of Mn^{2+} were incubated for 18 h at 23 °C, and reconstituted factor VIII activity was measured by the factor Xa generation assay as described in Materials and Methods. Each point represents the average value of quadruplicate samples. Lines were drawn from the curve fit according to a single-site binding model (eq 3) as described in Materials and Methods.

Effect of Mn^{2+} on the Binding of Ca^{2+} to Factor VIII as Determined by Equilibrium Dialysis. Since both Ca^{2+} and Mn^{2+} support the regeneration of active factor VIII to similar extents, an experiment was performed to determine whether the metal ions competed with one another for binding to the protein. Factor VIII (8 μM) was reacted in the presence of 20 μM free Ca^{2+} to yield ~ 0.5 mol Ca^{2+} bound per mole factor VIII. This Ca^{2+} concentration was selected so as to maximize the sensitivity for the competitive binding experiment. Subsequently, the reaction mixtures were titrated with varying concentrations of Mn^{2+}, and residual bound Ca^{2+} was determined. Up to 1 mM Mn^{2+} did not cause a significant reduction in the Ca^{2+} binding to factor VIII (data not shown). An estimated K_i of >1 mM for the competing Mn^{2+} was determined, and this value indicates a much weaker affinity than the Mn^{2+} binding affinity obtained by factor Xa generation assay ($K_d = 5.7 \pm 2.1$ μM). This result indicates that the high-affinity Ca^{2+} binding site (8.9−18.9 μM, stoichiometry = 1 Ca^{2+}/Factor VIII, ref *19*) differs from the Mn^{2+} binding site on factor VIII. Interestingly, inclusion of a saturating levels of both Ca^{2+} and Mn^{2+} did not result in a significant increase in activity as compared with Mn^{2+} alone (data not shown), suggesting no additive effect of the divalent metal ions.

Association of Factor VIII Subunits in the Presence of Mn^{2+} as Determined by Fluorescence Energy Transfer. The above results indicate that Mn^{2+} associates with high affinity to nonidentical site(s) as compared with Ca^{2+} yielding a somewhat greater specific cofactor activity. While Ca^{2+} was previously found to have no effect on the interfactor VIII chain affinity, the effect of Mn^{2+} on this parameter was not known. Therefore, the influence of Mn^{2+} on the association of HC and LC was determined by a series of experiments using fluorescence energy transfer between an Ac-LC (fluorescence donor) and an Fl-HC (fluorescence acceptor). Figure 3 shows the reduction of the relative fluorescence from acrylodan bound to LC as titrated with fluorescein-labeled HC in the presence of 20 mM Mn^{2+}. Unlabeled HC had little if any effect on the fluorescence intensity of Ac-LC (data not shown). The estimated affinity as determined by donor fluorescence quenching (K_d = 53.0 ± 17.1 nM)

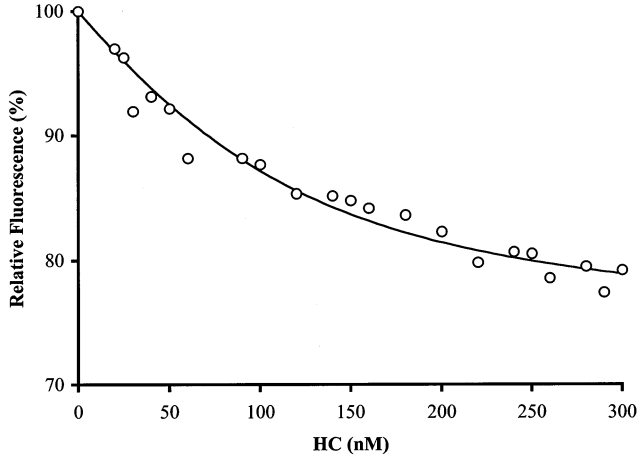

FIGURE 3: Donor fluorescence quenching as a result of subunit reassociation at equilibrium in the presence of 20 mM Mn^{2+}. Fluorescence energy transfer experiments were conducted using 100 nM acrylodan-labeled LC and 0−300 nM fluorescein-labeled HC in the presence of 20 mM Mn^{2+} as described in Materials and Methods. The relative fluorescence value represents a ratio of fluorescence intensity of Ac-LC in the presence of Fl-HC divided by the fluorescence intensity of Ac-LC alone. Fluorescence intensity values were integrated over a wavelength range of 460−490 nm. Each point represents the average value of six samples. The line was drawn by curve fitting using the equation as described in Materials and Methods.

was essentially identical to the affinity values previously obtained in the absence of metal ion ($K_d = 53.8 \pm 14.2$ nM) or in the presence of 25 mM Ca^{2+} ($K_d = 48.7 \pm 15.4$ nM) (*18*). Furthermore, the relative fluorescence at saturation of Ac-LC by Fl-HC in the presence of 20 mM Mn^{2+} (73.8 ± 2.1%) was indistinguishable from the value we previously obtained in the presence of 25 mM Ca^{2+} (73.5 ± 2.0%) and differed from that obtained in the presence of a low concentration of EDTA (79.3 ± 1.4%) (*18*). These results indicate that, similar to Ca^{2+}, Mn^{2+} does not have a physical effect on the affinity of factor VIII HC for LC, yet yields an equivalent interfluorophore separation between labeled residues in the HC and LC.

Tb^{3+} Binding to Factor VIII Subunits and Phosphorescence from Tb^{3+}−Factor VIII Subunit Complexes. The sensitized phosphorescence from protein-bound Tb^{3+} was employed to further characterize the interaction of Mn^{2+} with isolated factor VIII subunits. In this series of experiments, the affinity of Tb^{3+} for isolated HC, LC, and the HC-derived A1 and A2 subunits was determined. Subsequently, competition of the Tb^{3+} phosphorescence by Mn^{2+} was examined to obtain information of the affinity of Mn^{2+} for the factor VIII subunits (see below). Results shown in Figure 4 demonstrate that the phosphorescence signals from factor VIII HC and LC (Figure 4A) and A1 and A2 subunits (Figure 4B) were increased in a dose-dependent manner with the concentration of Tb^{3+}, and this binding was saturable. Some variation in the number of binding sites, binding affinity, and maximum Tb^{3+} phosphorescence were observed for the factor VIII subunits. Titration of HC, LC, and A2 by Tb^{3+} showed binding patterns in which a two-site Tb^{3+} binding pattern was supported by a *F*-test with high statistical significance (Table 1, $P < 0.01$). On the other hand, there was no significant improvement in the goodness-of-fit for a two-site binding model (eq 5) for A1 (Table 1, $P > 0.05$). A high-affinity Tb^{3+} binding site was detected for the A2

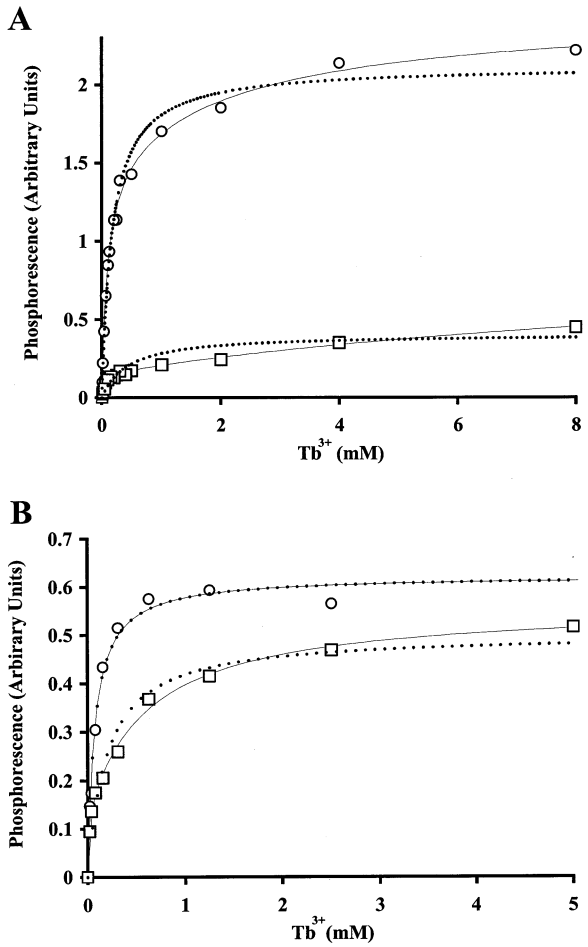

FIGURE 4: Tb^{3+} binding to factor VIII subunits. The change in phosphorescence at 538−556 nm from Tb^{3+}-bound HC and LC (open circles and squares, respectively, in panel A) and A1 and A2 subunits (open circles and squares, respectively, in panel B) were measured following an 18-h incubation with the indicated concentrations of Tb^{3+} as described in Materials and Methods. The phosphorescence values were normalized on a per micromolar protein concentration basis. Each point represents the average value from three independent measurements. Lines were drawn from the curve fit according to a single-site binding model (eq 4, dashed line) and a two-site binding model (eq 5, solid line) as described in Materials and Methods.

subunit ($K_d = 10.7$ μM), while sites showing more moderate affinity for Tb^{3+} were identified on A1, HC, and LC (K_d = 58.5−90.8 μM). Interestingly, Tb^{3+} showed an inhibitory effect on factor VIII activity (results not shown). The mechanism(s) for this inhibition are not fully understood. However, analyses employing fluorescence energy transfer suggested that the ion promotes dissociation of the factor VIII heterodimer (results not shown).

Observed intensities of the phosphorescence signals at saturating concentrations of Tb^{3+} markedly differed for the isolated factor VIII subunits examined. These effects were likely contributed, in part, by the local environment surrounding the Tb^{3+} binding site. For example, the simple addition of the maximum phosphorescence values from the high-affinity sites on A1 and A2 (0.621 + 0.14) was substantially less than the phosphorescence value from the high-affinity site on HC (1.54). This observation may be a reflection of the changes in conformation that occur with cleavage of the HC in yielding the individual A1 and A2 subunits (*21*, *27*). Alternatively, the phosphorescence from

Table 1: Estimated Tb^{3+} Binding Parameters on Factor VIII Subunits as Determined by Sensitized Tb^{3+} Phosphorescence[a]

factor VIII subunits	K_{d1} (μM)	F_{max1}	K_{d2} (μM)	F_{max2}	F value	P value
HC	172 ± 16.0	2.12 ± 0.05		0.933 ± 0.113	4.72	<0.005
	90.8 ± 15.2	1.54 ± 0.15	2408 ± 1417			
LC	427 ± 104	0.405 ± 0.032		0.809 ± 0.278	15.2	<0.0001
	58.5 ± 14.1	0.162 ± 0.017	14 127 ± 7867			
A1	75.5 ± 9.0	0.621 ± 0.017		0.311[b]	0.99	>0.05
	75.6[b]	0.311[b]	75.5[b]			
A2	194 ± 42.0	0.500 ± 0.027		0.420 ± 0.026	11.6	<0.01
	10.7 ± 8.3	0.140 ± 0.032	615 ± 143			

[a] Parameter values were calculated by nonlinear least-squares regression on the data shown in Figure 4 using the equation shown in Materials and Methods. The *F*-test was performed to compare and identify the better curve fit. The values in the first and second row in each data set were obtained from the curve fits using the one-site binding model and the two-site binding model, respectively. [b] Standard deviation >10 000.

Table 2: Estimated Mn^{2+} Binding Parameters on Factor VIII Subunits as Determined by the Inhibition of Sensitized Tb^{3+} Phosphorescence[a]

factor VIII subunits	K_{i1}(μM)	K_{i2} (μM)	α^b
HC	169 ± 40	251 ± 55	0.554 ± 0.041
LC	181 ± 26	583 ± 115	0.556 ± 0.053
A1	297 ± 84	475 ± 139	0.585 ± 0.055
A2	477 ± 140	1147 ± 447	0.909 ± 0.044

[a] Parameter values were calculated by nonlinear least-squares regression of the data shown in Figure 5 using the equation shown in Materials and Methods. [b] α is the phosphorescence ratio of both the Tb^{3+}- and the Mn^{2+}-bound subunits over the Tb^{3+}-bound subunit.

Tb^{3+} bound to HC may be enhanced by additional energy transfer from fluorescence donor residues (e.g., tryptophan residues) residing in the contiguous A domains. On the other hand, the small F_{max} value (0.162) observed for Tb^{3+} bound to the high-affinity site in LC suggested that this site was removed from any regions of clustered tryptophan residues. In both the HC and LC, the K_d values for the low-affinity Tb^{3+} binding sites were large (2.4−14 mM). Considering that the trivalency of Tb^{3+} lends itself to potentially higher-affinity interactions with protein as compared with divalent metal ions (*28*), this observation suggests that the putative role for these sites in specific metal binding may not be significant.

Mn^{2+} Binding to Factor VIII Subunits Detected by Inhibition of Tb^{3+} Phosphorescence from Tb^{3+}−Factor VIII Subunit Complexes. The sensitized phosphorescence from Tb^{3+} bound to the above factor VIII chains and subunits was used to monitor the association of Mn^{2+} with these factor VIII components. Use of intact factor VIII in this analysis was precluded by the apparent capacity of Tb^{3+} to facilitate separation of HC and LC (data not shown). The presence of Mn^{2+} attenuated phosphorescence, and the extent of this decrease was saturable and dependent upon the concentration of the metal ion (Figure 5). The inhibition of Tb^{3+}-phosphorescence by Mn^{2+} was used to estimate the affinity for Mn^{2+} binding to the subunit, according to the general model of enzyme inhibition (eq 6) described in Materials and Methods. As shown in Table 2, the K_{i1} and K_{i2} values obtained for the subunits varied somewhat but were within a range from ∼0.15 to 1 mM. This result suggested that the Mn^{2+}-dependent mechanism for inhibition of Tb^{3+} binding to the factor VIII subunits was neither a simple competitive nor simple indirect mode but rather a mixed-type inhibition. Comparison of the values for K_{i1} and K_{i2} (Table 2) suggested that Mn^{2+} binds with somewhat higher affinity to Tb^{3+} free protein than to Tb^{3+}-bound protein. Values for K_{i1} and K_{i2} obtained for the HC and derived subunits showed marginal differences as compared with the values obtained for LC, suggesting relatively weaker competition of Tb^{3+} for Mn^{2+} binding with HC derived subunits. The possible mechanism of this inhibition is that Mn^{2+} binding to the site in factor VIII subunits induces conformational change, which causes both the decrease in affinity of Tb^{3+} binding and the reduction of specific phosphorescence from Tb^{3+} bound to factor VIII. Interestingly, Ca^{2+} (up to 10 mM) did not cause any reduction of phosphorescence from Tb^{3+} bound to factor VIII subunits (results not shown), suggesting that Ca^{2+} was either not an effective competitor for Tb^{3+} and/or that Tb^{3+} did not occupy the Ca^{2+} binding sites in the subunits. This conclusion was supported by an experiment demonstrating the absence of competition for Ca^{2+}-bound factor VIII by Tb^{3+} using equilibrium dialysis (results not shown).

The curve fitting allows for calculation of a ratio, referred to as the α value, representing the intensity for the protein−Tb^{3+}−Mn^{2+} complex divided by the intensity for the protein−Tb^{3+} complex. The α values were similar for HC, LC, and A1 (0.554−0.585), indicating that Mn^{2+} was relatively effective in the quenching of Tb^{3+} phosphorescence. Similar affinity values for Tb^{3+} sites were identified using those factor VIII components. The high α value obtained for the isolated A2 subunit (0.909) suggested little (∼10%) quenching of Tb^{3+} phosphorescence by Mn^{2+}. This result may reflect the high-affinity Tb^{3+} site identified in the A2 subunit. Reasons for the inability of Mn^{2+} to completely displace bound Tb^{3+} are not well understood and may reflect a combination of effects including association of Tb^{3+} at regions in the protein other than Mn^{2+}-specific sites. Indeed, residual Tb^{3+} bound to protein in the presence of excess metal ion competitors have been observed in several systems (*29, 30*).

DISCUSSION

A study of the interactions of Mn^{2+} with factor VIII (subunits) was undertaken to clarify the role of this metal ion in generating functional factor VIII following reconstitution of the cofactor from its isolated subunits. Titration of factor VIII with Mn^{2+} followed by factor Xa generation assay indicated the presence of a high-affinity site on factor VIII (K_d = 5.7 ± 2.1 μM), as well as suggested the presence of lower-affinity sites. Furthermore, Mn^{2+} failed to increase the interchain affinity as detected by assessing the reconstitution of factor VIII by fluorescence energy transfer. While these results are qualitatively similar to

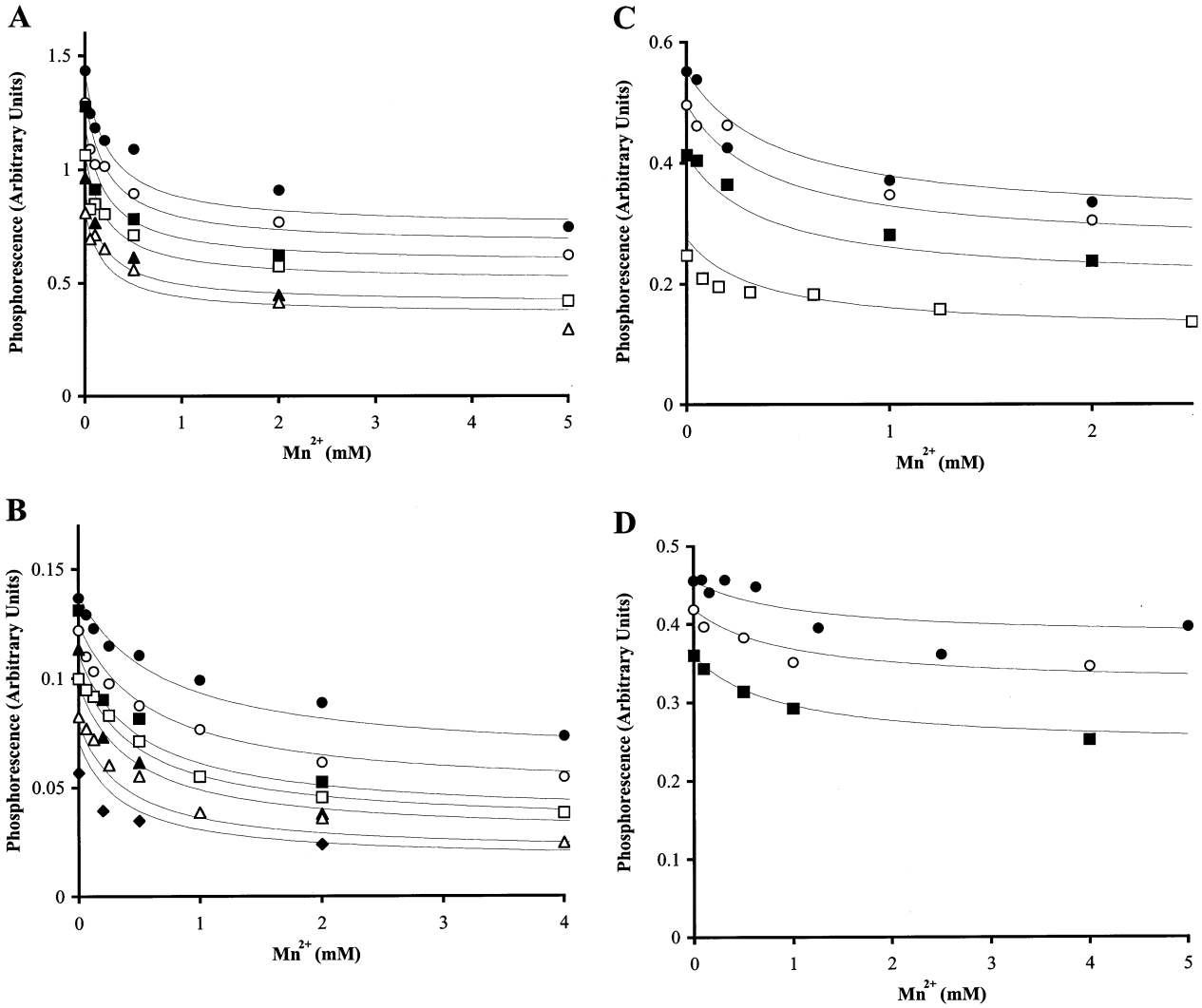

FIGURE 5: Inhibition of Tb^{3+} phosphorescence from factor VIII subunits by Mn^{2+}. The change in phosphorescence at 538−556 nm from Tb^{3+}-bound HC (panel A), LC (panel B), A1 (panel C), and A2 (panel D) were measured after 18 h incubation with the fixed amount of Tb^{3+} in the presence of the indicated concentrations of Mn^{2+} as described in Materials and Methods. The phosphorescence values were normalized on a per micromolar protein concentration basis. Each point represents the average value from three independent measurements. Lines were drawn by the curve fitting according to the model (eq 6) as described in Materials and Methods. The concentrations of Tb^{3+} employed in panel A are 1000, 500, 300, 200, 125, and 100 μM (closed circles, open circles, closed squares, open squares, closed triangles, and open triangles, respectively); those in panel B are 500, 250, 150, 125, 100, 62.5, and 50 μM (closed circles, open circles, closed squares, open squares, closed triangles, open triangles, and closed diamonds, respectively); those in panel C are 600, 300, 150, and 60 μM (closed circles, open circles, closed squares, and open squares, respectively); and those in panel D are 2000, 1000, and 500 μM (closed circles, open circles, and closed squares, respectively).

properties attributed to Ca^{2+}, competition experiments employing $^{45}Ca^{2+}$ equilibrium dialysis and displacement of protein-bound Tb^{3+} indicated that the Mn^{2+} binding site(s) in factor VIII is (are) different from the Ca^{2+} binding site(s). Thus, Mn^{2+} likely generates factor VIII cofactor activity by a similar mechanism as observed for Ca^{2+}, although through interaction at nonidentical sites.

Early studies examining the association of the HC and LC of factor VIII (*12*, *13*) and the homologous protein, factor Va (*16*, *31*), indicated the capacity of both Ca^{2+} and Mn^{2+} to facilitate reconstitution of functional protein. Subsequent studies using factor Va clarified that the role of Ca^{2+} was to markedly increase the interchain affinity (*17*, *32*), as well as modulate modest conformational changes in the reassociated heterodimer that correlated with the generation of activity (*33*). While Ca^{2+} also appears to alter the conformation of the factor VIII heterodimer, on the basis of changes in interfluorophore spatial separation of labeled chains as assessed by fluorescence energy transfer, it makes no contribution to the interchain affinity (*18*). Effects of Mn^{2+} on the structure and activity of the cofactors have been less well-studied but are presumed to function in a manner similar to Ca^{2+}. Interestingly, cofactor activities regenerated in the presence of Mn^{2+} appear somewhat greater (∼50−100%) than those observed for Ca^{2+} (*12*, *16*, *31*), suggesting that the metal ion-dependent changes in conformation correlating with formation of active material are similar but not identical. We also observed in this study that occupancy of the high-affinity Mn^{2+} site in factor VIII was sufficient to generate near maximal levels of cofactor activity. This result differs somewhat from our recent observation on the binding of Ca^{2+} to factor VIII and correlation of activity generation (*19*). In that study, occupancy of the high-affinity site ($K_d = 8.9$ μM) yielded an intermediate specific activity that was ∼40% of

maximal. Maximal levels of cofactor activity were generated only following Ca^{2+} binding to both the high and the low (K_d = 4 mM) sites. Thus, subtle differences exist in the interactions of the metal ions with the cofactor and resultant effects on activity.

Disparate effects of Mn^{2+} and Ca^{2+} on the structure of factor VIII and isolated subunits have been observed. While Ca^{2+} showed no detectable effect on the secondary structure of factor VIII or isolated HC and LC (*34*), modest changes in HC and LC were observed in the presence of Mn^{2+} (*15*). Furthermore, marked differences in thermal denaturation profiles of factor VIII LC were detected using extrinsic fluorescence of the protein-bound, apolar probe, bis-anilinonaphthalsulfonic acid in response to the ions (*15*). While Mn^{2+} showed a low intensity, biphasic thermal transition (T_m values of 47 and 59 °C), Ca^{2+} yielded a sharp, single-phase transition. This latter response was similar to the single-phase thermal transition observed for LC in the absence of metal ions (T_m values of 50.5 and 53 °C in the absence and presence of Ca^{2+}, respectively). Thus, it is tempting to speculate that these structural differences may give rise to the altered activity values observed in the reconstituted cofactors.

Tb^{3+} is a trivalent metal ion of the lanthanide series. Since the effective ionic radius of Tb^{3+} (0.92 Å) is similar to that of Ca^{2+} (0.99 Å), this metal ion has often been used for probing the Ca^{2+} binding site (*28*). Interestingly, we observed that in the case of factor VIII, Ca^{2+} (>10 mM) did not show significant inhibition of Tb^{3+} phosphorescence on factor VIII subunits, while Tb^{3+} did not compete with Ca^{2+} for factor VIII binding as judged by equilibrium dialysis. However, Mn^{2+} inhibited the Tb^{3+} binding to factor VIII subunits by a mixed-type inhibition pattern with somewhat greater contribution from the competitive element as compared with the indirect element. Values for the affinity of Mn^{2+} with the isolated chains and subunits of factor VIII obtained by this Tb^{3+}-competiton approach (based on K_i values) were significantly greater than the high-affinity K_d values determined for the intact heterodimer using the functional assays. This disparity may indicate that the high-affinity site requires association of HC and LC and is not manifested on the isolated chains. Alternatively, association of Tb^{3+} may alter the conformation of the subunits thereby affecting Mn^{2+} site(s) and reducing the affinity for the metal ion.

Although Tb^{3+} was of some utility in characterizing interactions of Mn^{2+} with various factor VIII subunits, its applications were limited to structural assays. This is because low (μM) concentration of Tb^{3+} inhibited factor VIII activity. The mechanism for inhibition likely resulted from dissociation of the factor VIII HC and LC as suggested by fluorescence energy transfer studies. This result could derive from Tb^{3+} competing for the $Cu^{+/2+}$ binding site since occupancy of this site by $Cu^{+/2+}$ results in a 100-fold increase in the interfactor chain affinity (K_d ~0.5 nM vs ~50 nM in the presence and absence of $Cu^{+/2+}$, respectively, ref *18*). Thus, occupancy of this site by Tb^{3+} may disrupt the binding interaction between HC and LC facilitating chain separation. Tb^{3+} was also observed to bind to factor VIII subunits in a manner that was resistant to competition by Mn^{2+}, as judged by significant levels of the lanthanide persisting in the presence of saturating levels of Mn^{2+}. These high levels of residual Tb^{3+} were particularly apparent in experiments using the A2 subunit of factor VIII. Given that this subunit contains critical interactive sites for factor IXa (*35*, *36*) and is essential for factor VIII function (*37*, *38*), association of residual Tb^{3+} at important interactive sites could also attenuate cofactor activity.

The ligands for the coordination of Ca^{2+} are usually carboxyl oxygen atoms from acidic amino acid side chains (*39*). While Mn^{2+}−ligand complexes are relatively weaker in general than those formed with other metal ions, they are typically stronger than those formed with Ca^{2+} or Mg^{2+} and are coordinated by carboxyl oxygen atoms from acidic amino acids plus imidazole nitrogen atoms from His residues (*40*). Observations that Mn^{2+} and Ca^{2+} did not compete with one another in binding factor VIII suggests that coordination of the former ion involves residues other than solely acidic amino acids. One interesting possibility is that, according to the ceruloplasmin-based factor VIII homology model (*41*), three His residues (H99, H161, and H314) reside in close proximity to the putative Ca^{2+} binding site (*19*) based in part on the data obtained for a homologous region in factor V (residues 94−110) (*42*). Thus, it is interesting to speculate that Mn^{2+} is coordinated by these His residues and the acidic amino acids from this region (residues 108−124). If so, it would suggest that Ca^{2+} and Mn^{2+} affect the same region of the cofactor through nonidentical but adjacent sites, and this interaction would represent a key role in the generation of cofactor activity. Furthermore, a shared site that is occupied by either Ca^{2+} or Mn^{2+} is also consistent with observations that there is no additive effect when cofactor activity in measured in the presence of both Ca^{2+} and Mn^{2+}.

In summary, the above results, taken together with our earlier studies on the roles of metal ions in factor VIII (*15*, *18*, *19*), suggest the following model. The single Cu ion identified in factor VIII appears to facilitate subunit association and maintain the heterodimer structure. However, this ion is auxiliary to activity generation. Ca^{2+} and Mn^{2+} likely interact at multiple, nonidentical but possibly spatially adjacent sites within the heterodimer. While these interactions do not affect the interfactor VIII chain affinity, their association appears to differentially alter heterodimer structure yielding active cofactor conformations.

ACKNOWLEDGMENT

We thank Dr. Lisa Regan of the Bayer Corporation and Debbie Pittman of the Genetics Institute for the gifts of recombinant human factor VIII. We also thank Drs. Charles W. Francis and Abha Sahni and Carrie-Ann Ballard for assistance in experiments involving radioisotopes.

REFERENCES

1. Davie, E. W. (1995) *Thromb. Haemostasis 74*, 1−6.
2. Lollar, P. (1995) *Adv. Exp. Med. Biol. 386*, 3−17.
3. Wood, W. I., Capon, D. J., Simonsen, C. C., Eaton, D. L., Gitschier, J., Keyt, B., Seeburg, P. H., Smith, D. H., Hollingshead, P., Wion, K. L., Delwart, E., Tuddenham, E. D. G., Vehar, G. A., and Lawn, R. M. (1984) *Nature 312*, 330−37.
4. Toole, J. J., Knopf, J. L., Wozney, J. M., Sultzman, L. A., Buecker, J. L., Pittman, D. D., Kaufman, R. J., Brown, E., Shoemaker, C., Orr, E. C., Amphlett, G. W., Foster, W. B., Coe, M. L., Knutson, G. J., Fass, D. N., and Hewick, R. M. (1984) *Nature 312*, 342−47.

5. Vehar, G. A., Keyt, B., Eaton, D., Rodriguez, H., O'Brien, D. P., Rotblat, F., Oppermann, H., Keck, R., Wood, W. I., Harkins, R. N., Tuddenham, E. G. D., Lawn, R. M., and Capon, D. J. (1984) *Nature 312*, 337−42.
6. Fass, D. N., Knutson, G. J., and Katzmann, J. A. (1982) *Blood 59*, 594−600.
7. Andersson, L. O., Forsman, N., Huang, K., Larsen, K., Lundin, A., Pavlu, B., Sandberg, H., Sewerin, K., and Smart, J. (1986) *Proc. Nat. Acad. Sci. U.S.A. 83*, 2979−83.
8. Fay, P. J., Anderson, M. T., Chavin, S. I., and Marder, V. J. (1986) *Biochim. Biophys. Acta 871*, 268−78.
9. Church, W. R., Jernigan, R. L., Toole, J., Hewick, R. M., Knopf, J., Knutson, G. J., Nesheim, M. E., Mann, K. G., and Fass, D. N. (1984) *Proc. Nat. Acad. Sci. U.S.A. 81*, 6934−7.
10. Bihoreau, N., Pin, S., Kersabiec, A. M. D., Vodot, F., and Fontaine-Aupart, M. P. (1994) *Eur. J. Biochem. 220*, 41−48.
11. Tagliavacca, L., Moon, N., Dunham, W. R., and Kaufman, R. J. (1997) *J. Biol. Chem. 272*, 27428−34.
12. Fay, P. J. (1988) *Arch. Biochem. Biophys. 262*, 525−31.
13. Nordfang, O., and Ezban, M. (1988) *J. Biol. Chem. 263*, 1115−8.
14. Fay, P. J., and Smudzin, T. M. (1989) *J. Biol. Chem. 264*, 14005−10.
15. Sudhakar, K., and Fay, P. J. (1998) *Biochemistry 37*, 6874−82.
16. Esmon, C. T. (1979) *J. Biol. Chem. 254*, 964−73.
17. Krishnaswamy, S., Russell, G. D., and Mann, K. G. (1989) *J. Biol. Chem. 264*, 3160−8.
18. Wakabayashi, H., Koszelak, M. E., Mastri, M., and Fay, P. J. (2001) *Biochemistry 40*, 10293−300.
19. Wakabayashi, H., Schmidt, K. M., and Fay, P. J. (2002) *Biochemistry 41*, 8485−92.
20. Mimms, L. T., Zampighi, G., Nozaki, Y., Tanford, C., and Reynolds, J. A. (1981) *Biochemistry 20*, 833−40.
21. Fay, P. J., Mastri, M., Koszelak, M. E., and Wakabayashi, H. (2001) *J. Biol. Chem. 276*, 12434−9.
22. Tsien, R. Y. (1980) *Biochemistry 19*, 2396−404.
23. Linse, S., Helmersson, A., and Forsen, S. (1991) *J. Biol. Chem. 266*, 8050−4.
24. Lollar, P., Fay, P. J., and Fass, D. N. (1993) *Methods Enzymol. 222*, 128−43.
25. Schiodt, J., Harrit, N., Christensen, U., and Petersen, L. C. (1992) *FEBS Lett. 306*, 265−8.
26. Kuby, S. A. (2000) *A study of Enzymes: Enzyme catalysis, kinetics, and substrate binding*, pp 1−56, CRC Press, Boca Raton, FL.
27. O'Brien, L. M., Huggins, C. F., and Fay, P. J. (1997) *Blood 90*, 3943−50.
28. Martin, R. B., and Richardson, F. S. (1979) *Q. Rev. Biophys. 12*, 181−209.
29. Hadad, N., Zable, A. C., Abramson, J. J., and Shoshan-Barmatz, V. (1994) *J. Biol. Chem. 269*, 24864−9.
30. Dickeson, S. K., Bhattacharyya-Pakrasi, M., Mathis, N. L., Schlesinger, P. H., and Santoro, S. A. (1998) *Biochemistry 37*, 11280−8.
31. Nesheim, M. E., Foster, W. B., Hewick, R., and Mann, K. G. (1984) *J. Biol. Chem. 259*, 3187−96.
32. Guinto, E. R., and Esmon, C. T. (1982) *J. Biol. Chem. 257*, 10038−43.
33. Laue, T. M., Lu, R., Krieg, U. C., Esmon, C. T., and Johnson, A. E. (1989) *Biochemistry 28*, 4762−71.
34. Sudhakar, K., and Fay, P. J. (1996) *J. Biol. Chem. 271*, 23015−21.
35. Fay, P. J., Beattie, T., Huggins, C. F., and Regan, L. M. (1994) *J. Biol. Chem. 269*, 20522−7.
36. Bajaj, S. P., Schmidt, A. E., Mathur, A., Padmanabhan, K., Zhong, D., Mastri, M., and Fay, P. J. (2001) *J. Biol. Chem. 276*, 16302−9.
37. Fay, P. J., Haidaris, P. J., and Smudzin, T. M. (1991) *J. Biol. Chem. 266*, 8957−62.
38. Lollar, P., and Parker, E. T. (1991) *J. Biol. Chem. 266*, 12481−6.
39. Martin, R. B. (1984) *Calcium and its role in biology*, Vol. 17, Marcel Dekker, Inc., New York.
40. Weatherburn, D. C. (2001) in *Handbook on metalloproteins* (Bertini, I., Sigel, A., and Sigel, H., Eds.) pp 193−268, Marcel Dekker, Inc., New York.
41. Pemberton, S., Lindley, P., Zaitsev, V., Card, G., Tuddenham, E. G., and Kemball-Cook, G. (1997) *Blood 89*, 2413−21.
42. Zeibdawi, A. R., and Pryzdial, E. L. (2001) *J. Biol. Chem. 276*, 19929−36.

BI026430E